Open Archive TOULOUSE Archive Ouverte (OATAO)

OATAO is an open access repository that collects the work of Toulouse researchers and makes it freely available over the web where possible.

Influence of corrosion and creep on intergranular fatigue crack path in 2XXX aluminium alloys

Gilbert Hénaff *, Frédéric Menan [1], Grégory Odemer [2]

Institut Pprime, UPR 3346 CNRS – ENSMA – Université de Poitiers, Département Physique et Mécanique des Matériaux, ENSMA – Téléport 2, 1 Avenue Clément Ader, BP 40109, F-86961 Futuroscope Chasseneuil Cedex, France

A B S T R A C T

In this paper, two examples of the influence of time-dependent processes on crack path in two 2XXX aluminium alloys are presented. The first example is concerned with corrosion–fatigue crack growth resistance of a 2024 T351 alloy cracked in the S–L direction in 3.5% NaCl solution at free corrosion potential. The second example deals with the elevated temperature crack growth resistance of a 2650 T6 alloy that might be used in future supersonic aircraft fuselage panels. The common idea is to correlate quantitative measurements of relevant fractographic features of crack path to the effects of time-dependent processes on crack growth rates.

Aluminium alloy
Corrosion–fatigue
Creep–fatigue
Hydrogen embrittlement
Cavitation

1. Introduction

The demand for the extension of aircraft service life is increasing, both as regards the management of ageing air fleets and the design of aircraft next generation. Now the damage tolerance assessment of Aluminium alloy (AA) aerostructures is generally based on fatigue crack growth data that are derived from laboratory tests carried out at relatively high frequencies in order to shorten test duration. As a consequence, the extrapolation of these data to very long service lives must rely on an in-depth understanding of the crack growth process, especially of the role of time-dependent processes that might take place. Progress in this area can in particular be achieved through a detailed analysis of crack paths. In addition, in many practical instances, time-dependent processes such as creep or corrosion may affect crack tip deformation and damage mechanisms, and as a consequence they can modify the crack growth rates as well as the crack path. Reciprocally the analysis of crack paths can provide insights into the relevance of time-dependent processes during crack growth in actual components, in particular when a transition from transgranular to intergranular crack path is noticed.

As more specifically regards crack paths observed in Aluminium Alloys (AA) used in aircraft airframes, different cracking modes can be observed:

(1) The stage I cracking mode that corresponds with a crack propagating by shear within a persistent slip band, as observed in fatigued single crystals or during the early growth stage of a crack initiated at the free surface of a polycrystal [1,2];

---

* Corresponding author. Tel./fax: +33 5 49 49 82 38.
  E-mail address: gilbert.henaff@ensma.fr (G. Hénaff).
[1] Present address: Institut de Soudure, 4 Boulevard Henri Becquerel, 57970 Yutz, France.
[2] Present address: Cirimat, Ensiacet, 118 Route de Narbonne, 31077 Toulouse Cedex 04, France.

(2) The stage II propagation regime is observed when at least two slip systems along {1 1 1} planes are symmetrically activated at the crack tip, leading to rupture along a {1 0 0} plane; the macroscopic crack path is then perpendicular to the mode I stress axis [1,3];

(3) Finally a stage I like propagation mode can be observed in cases where ageing conditions promote the localisation of plastic deformation within a single slip system in individual grains; thus the propagation within a grain is comparable to a stage I mode, whereas the crack path at the macroscopic scale remains perpendicular to the mode I stress axis as in stage II [4,5].

These different regimes are schematically sketched in Fig. 1. While the propensity of a long crack to propagate along stage II or stage I like mode is partly intrinsic to the microstructure, it can also be largely altered by environmental effects. In particular, it has been shown that the presence of a small amount of water in the test atmosphere can induce a drastic change in crack path by shifting from a stage I like to a stage II regime [6]. It is furthermore noteworthy that all these characteristic regimes basically correspond to a transgranular cracking mode. However, in some alloys, the presence of a significant amount of intergranular facets within a mainly transgranular crack path has been reported in different alloys. This is in particular the case for quenched and tempered steels [7–10]. Decohesions along prior austenite grain boundaries are generally attributed to a form of hydrogen embrittlement taking place in the process zone, although the detailed mechanisms have not been fully elucidated. Nevertheless, this indicates that the effect of an extrinsic factor such as environment can alter the fundamental nature of the crack path.

As more specifically regards AA, intergranular cracking has been reported in crack initiation in pure aluminium [11] as well as in crack propagation during environmentally-assisted fatigue crack propagation fatigue [12,13], especially in high strength alloys. In the latter case, the occurrence of intergranular fracture has also been related to an embrittling effect of hydrogen diffusing along grain boundaries [14].

The present paper precisely reports on two examples of the occurrence of intergranular crack path induced by time-dependent processes in 2XXX AA. In the first example, the corrosion–fatigue crack growth behaviour in saline solution of a 2024 T351 AA used in many airframe components and here mainly cracked in the S-L orientation is examined at different frequencies. This study was actually undertaken in order to identify the propagation domains where synergistic effects between fatigue and corrosion might exist. In the second example, the fatigue crack growth behaviour of a 2650 AA that might be used in fuselage panels of the next generation of civil transport supersonic aircraft is investigated at elevated temperatures and low frequencies. Indeed, at a cruise speed of Mach 2, the fuselage skin will have to withstand temperatures in the range 100–130 °C for a total long duration. Thus the objective was to identify the possible interactions between fatigue and creep damage that might take place at the crack tip during propagation.

The common idea in these investigations is to examine if the extension of intergranular fracture could be correlated to the intensity of the effects of time-dependent processes on the crack growth mechanisms as characterised at the macroscopic scale by crack growth rates. At this aim, quantitative measurements of intergranular decohesions are performed for different testing conditions.

2. Corrosion–fatigue crack growth in 2024 T351 alloy

2.1. Material and experimental techniques

The material of the study is a 2024 aluminium alloy with nominal composition Cu 4.5%, Mg 1.4%, Mn 0.60%, Fe 0.13%, Si 0.06%, Ti 0.03%, Zr + Ti 0.03%, Al balance, in the temper condition T351. The average grain size is 90 μm, 210 μm and 820 μm
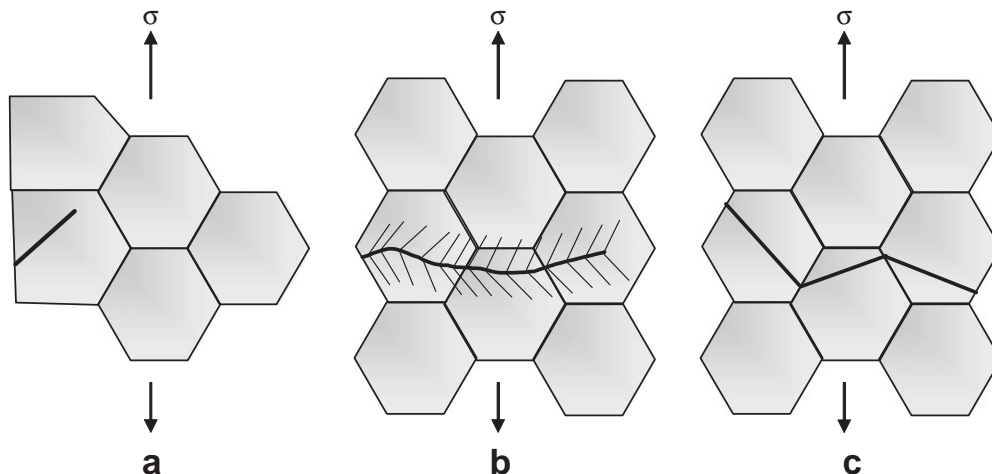

Fig. 1. Characteristic fatigue crack growth regimes reported in 2XXX aluminium alloys, namely (a) stage I, (b) stage II, and (c) stage I like.

in the short transverse S, long transverse T and laminate L direction, respectively. Compact Tension specimens W = 40 mm, thickness B = 10 mm have been machined in the S-L orientation from a 50 mm thick plate provided by EADS IW. The crack plane is located at mid thickness of the plate, where the cooling rate is slower and high corrosion susceptibility is expected. The environments considered in this study are: ultra-high vacuum (UHV) (10^{-7} mbar), laboratory air (20–30 °C), distilled water, permanent immersion in a saline solution composed of distilled water with 3.5% NaCl addition (pH = 7). Corrosion fatigue experiments were carried out under load control at free corrosion potential on a servo-hydraulic machine equipped with a Plexiglas cell. The selected value of the R load ratio was 0.7 in order to avoid crack closure effects. More details can be found elsewhere [15,16].

2.2. Results and analysis

The corrosion–fatigue crack growth rates in saline solution were measured at different frequencies in order to investigate the effect of time-dependent processes. The results are reported in Fig. 2 and compared to those obtained in UHV, air and distilled water. The characteristic fracture surfaces associated to these different loading and environmental conditions are presented in Fig. 3.

It is noteworthy that air and distilled water induce a significant fatigue crack growth enhancement with respect to ultra-high vacuum. This enhancement is associated with a shift from a predominant stage I like regime in UHV (Fig. 3a) to a stage II propagation in air and distilled water with a transgranular cleavage-like cracking mode (Fig. 3b and c) and the formation of dimples around coarse intermetallic particles, especially for high values of ΔK. It was previously proposed that this shift in air could be related to the effect of water vapour adsorption on crack tip surfaces [6]. Surface adsorption would modify the activity of dislocation sources around the crack tip [17] and, by this, would inhibit the intrinsic propensity to stage I like cracking. As regards the propagation in saline solution, a fatigue crack growth enhancement is observed at high frequencies, namely in the range 2.5–10 Hz, while crack growth rates measured at 0.1 Hz are comparable to those observed in air or in distilled water despite of the longer exposure duration to the corrosive medium. Actually, the results obtained under different loading wave shapes and presented in Fig. 4 indicate that the enhancement observed in saline solution is governed by the Rise Time (RT) [15]. This marked influence of RT on growth rates corresponds to two characteristic propagation regimes which are schematically represented in Fig. 5. In the crack growth rate domain considered, the behaviour in air, distilled water and saline solution under short RT loading is characterised by a 4th power law dependence of da/dN versus ΔK. In saline solution and under long RT loading, the growth rates are enhanced and obey to a 2nd power law. The plateau observed at 1 Hz may represent a transition between a 2nd power-law regime, where corrosion-assisted crack growth effects are relatively important, to a 4th power-law regime where the influence of environment is less pronounced.
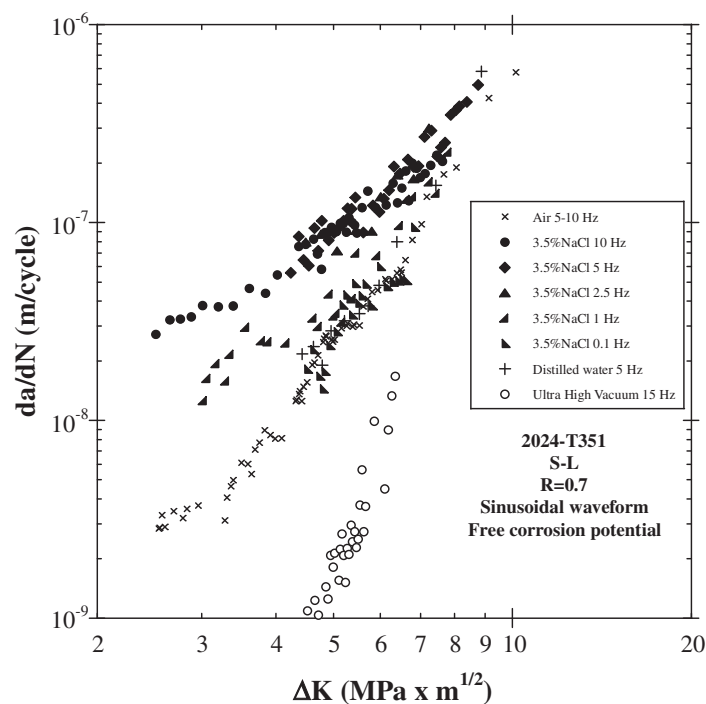

Fig. 2. Corrosion fatigue crack growth rates measured as a function of ΔK at different frequencies in saline solution in comparison with high vacuum, air and distilled water.
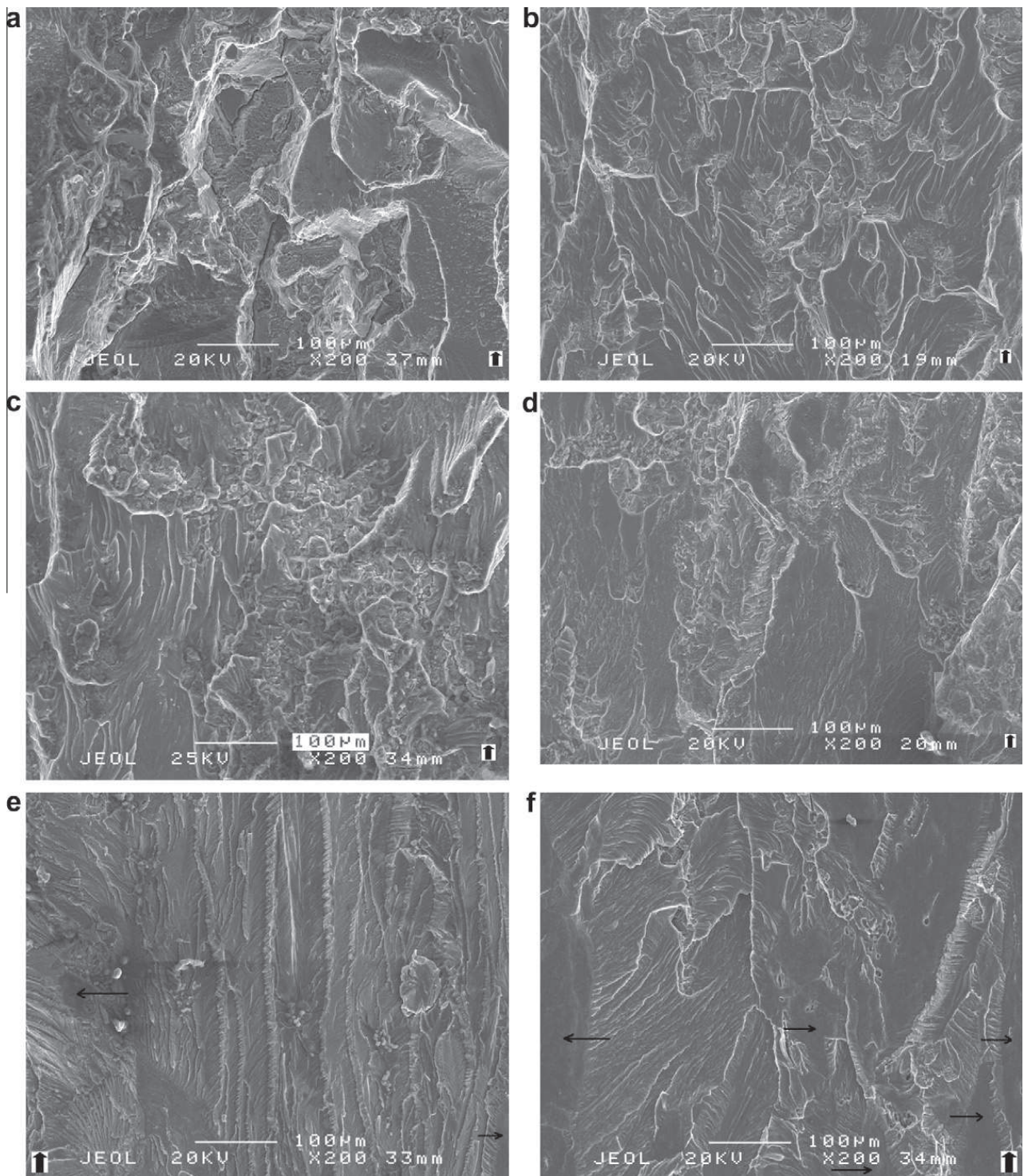
Fig. 3. Fatigue fracture surfaces produced at $\Delta K = 6$ MPa m$^{1/2}$ under sinusoidal waveform: (a) ultra-high vacuum 15 Hz, (b) air 5–10 Hz, (c) distilled water 5 Hz, (d) 3.5% NaCl solution 10 Hz; $\Delta K = 3$ MPa m$^{1/2}$, 10 Hz, (e) air, and (f) 3.5% NaCl (crack propagation from bottom to top).

The fracture surfaces produced in saline solution do not seem, at a first glance, fundamentally different from those obtained in air and distilled water. At lower ΔK values, however, the presence of some flat large smooth facets, showing no evidence of striations or cleavage steps, is noticed. These facets are pointed out by the small dark arrows in Fig. 3f. Such facets are also present in air but they are more numerous and larger (Fig. 3e and f) in saline solution.

In order to establish a possible relation between the activation of this corrosion-assisted regime and the amount of such facets, quantitative measurements of the fracture surface occupied by those facets have been performed. These data have been reported on a da/dN–ΔK graph in Fig. 6. The percentages of facets in 3.5% NaCl at 1 Hz with a sinusoidal waveform indicate that, in the 4th power-law regime, the crack growth enhancement can also be correlated with the increase in the area
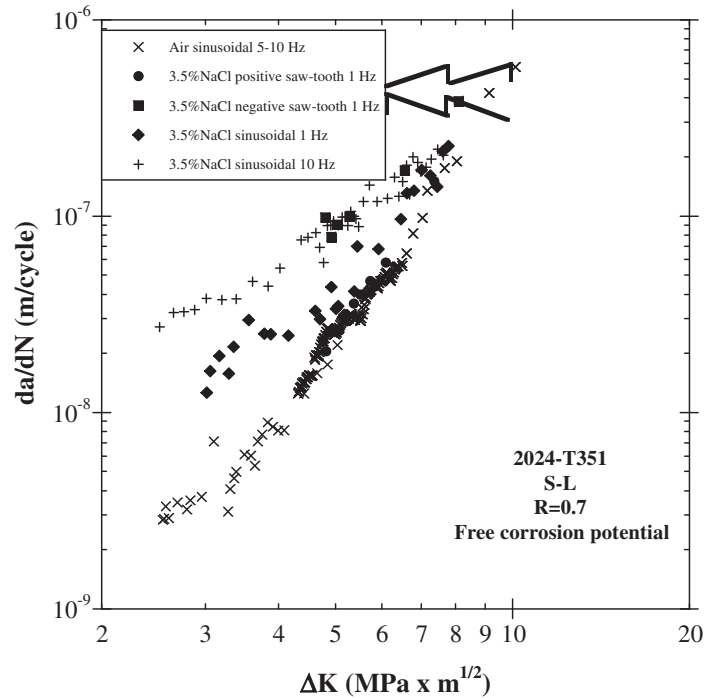
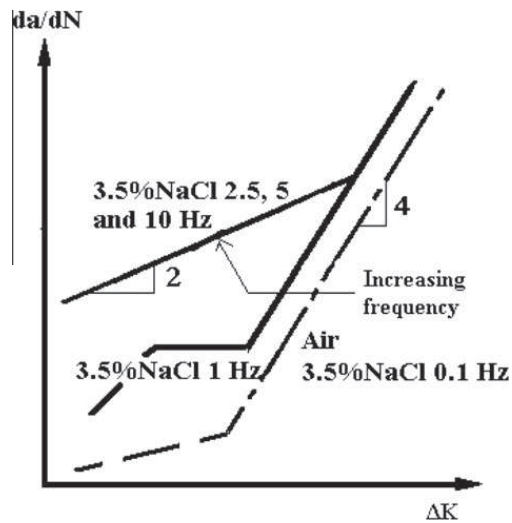**Fig. 4.** Influence of loading waveforms on corrosion–fatigue crack growth rates in saline solution.

Fig. 5. Influence of the loading frequency on the FCGRs of the alloy 2024 T351 for a sinusoidal waveform ($R = 0.7$, S-L orientation).

occupied by facets. Indeed, at $\Delta K = 4$ MPa m$^{1/2}$, the facets in air represent 2% of the total area, whereas the facets in saline solution at 1 Hz with a sinusoidal waveform represent 18% of the total surface area, with da/dN independent of the stress intensity range ($n = 0$, where n denotes the exponent of the power law) around this ΔK value. Therefore, the presence of facets cannot be considered as characteristic of the 2nd power-law regime, but this regime seems to promote the formation of facets. In order to identify the nature of the flat large smooth facets, etch pitting of the fracture surfaces has been realized. In saline solution, the shape of the etching pits is neither square (typical of near {1 0 0} crystallographic plane, as is shown in Fig. 7a in the case of crack propagation in air) nor triangle (typical of near {1 1 1} crystallographic plane). These pits may correspond to higher index planes not associated with a grain boundary. However, it should be noticed that different pit shapes are observed over a single facet (Fig. 7b), which does not support such an assumption. Hence the intergranular nature of these facets constitutes a reasonable hypothesis, which would furthermore be consistent with the morphology of these facets. Indeed the facets, indicated in the black boxes in Fig. 8b, exhibit a pancake shape and curved edges, similar to the morphology of the grains and to the fracture surface produced during dissolution-controlled intergranular stress corrosion cracking and presented in Fig. 8a.
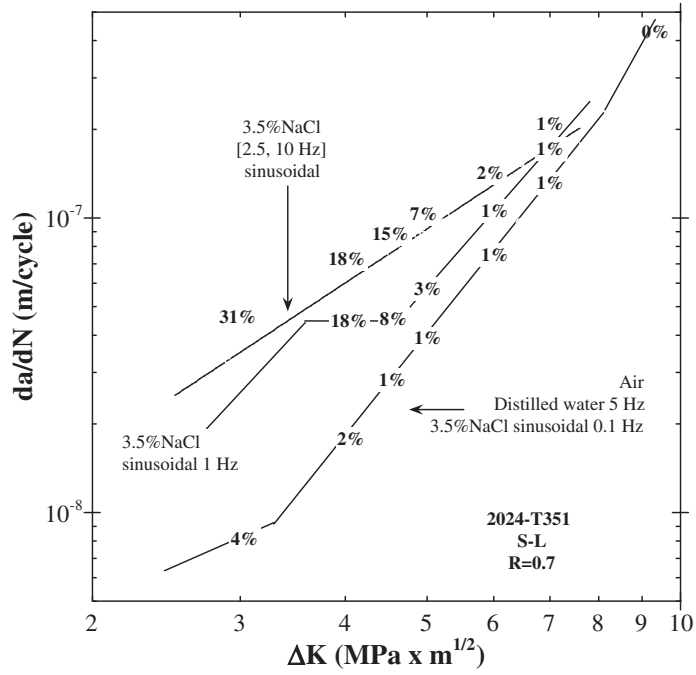
Fig. 6. Percentages of flat facets measured on fracture surfaces produced in the S-L orientation and reported in a *da/dN–ΔK* graph.
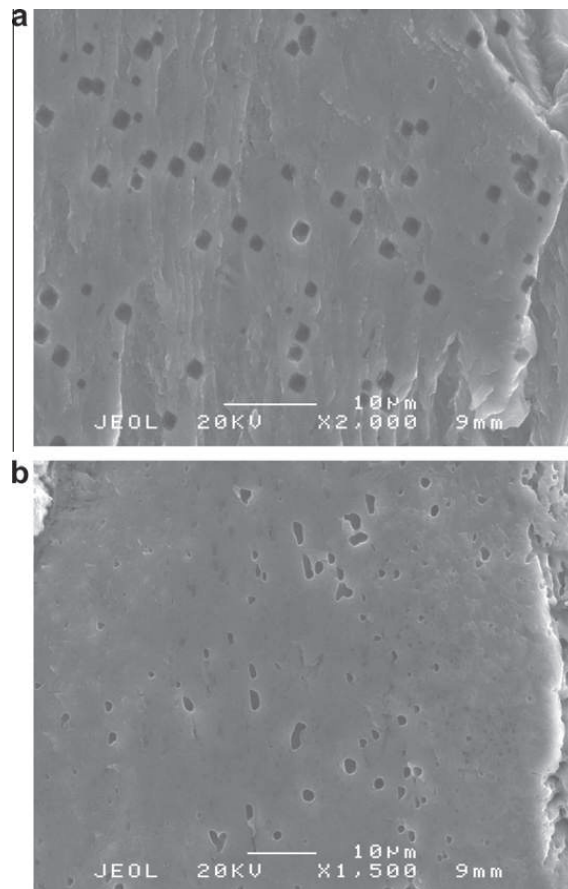

Fig. 7. Etch pit analysis of fracture surfaces. (a) Square etch pits observed on a fracture surface produced during fatigue crack propagation in air ($R = 0.7$, $\Delta K = 3$ MPa m$^{1/2}$) and indicating a crack path close to {1 0 0} planes and (b) identification of the flat, large and smooth facets in air and saline solution by Keller's reagent etch pitting ($R = 0.7$, 5 Hz, sinusoidal waveform, 3.5% NaCl, $\Delta K = 5.7$ MPa m$^{1/2}$).
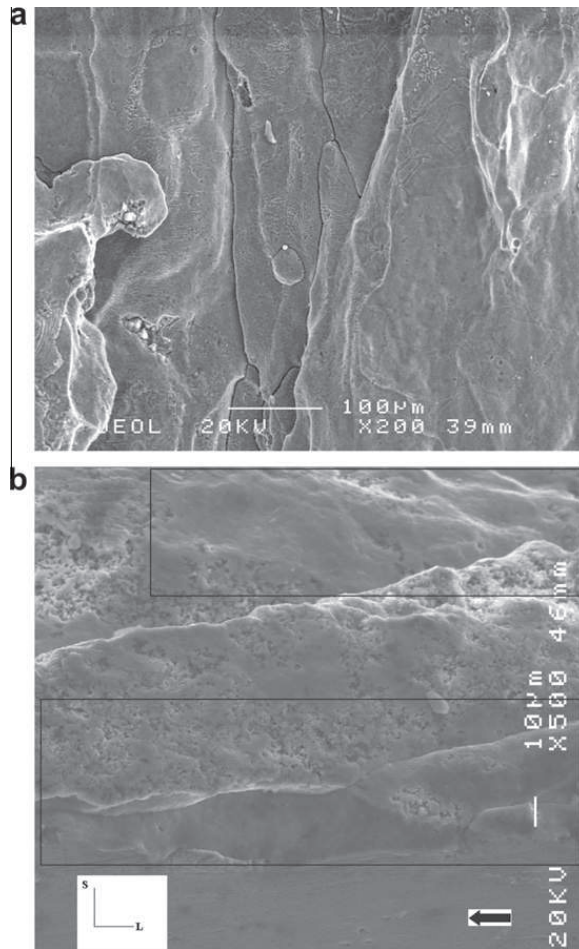
Fig. 8. (a) Intergranular fracture surface produced during stress corrosion cracking in the 2024 T351 alloy in the S-L orientation and (b) morphology of the facets produced in saline solution in the 2024 T351 alloy in the S-L orientation ($R = 0.7$, 10 Hz, ΔK = 4–4.5 MPa m$^{1/2}$). Black arrow: crack propagation direction.
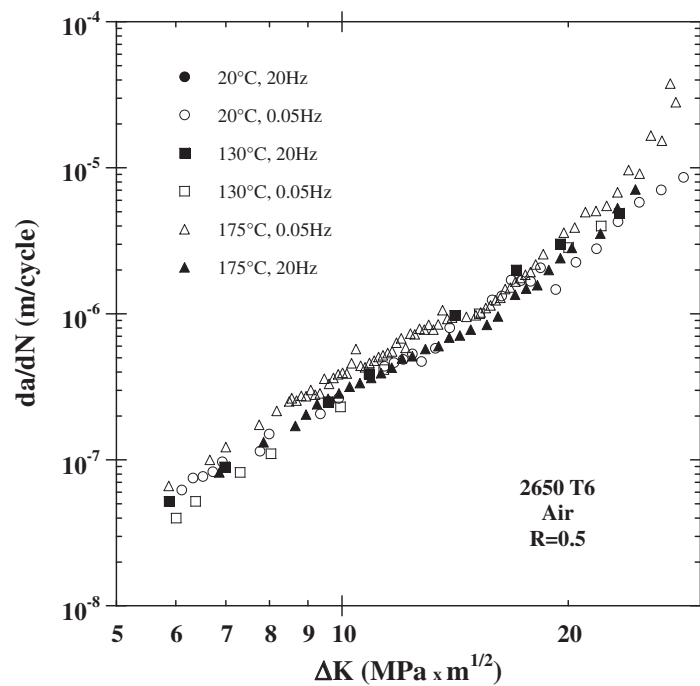

Fig. 9. Fatigue crack growth rates measured in air at different temperatures and different frequencies.
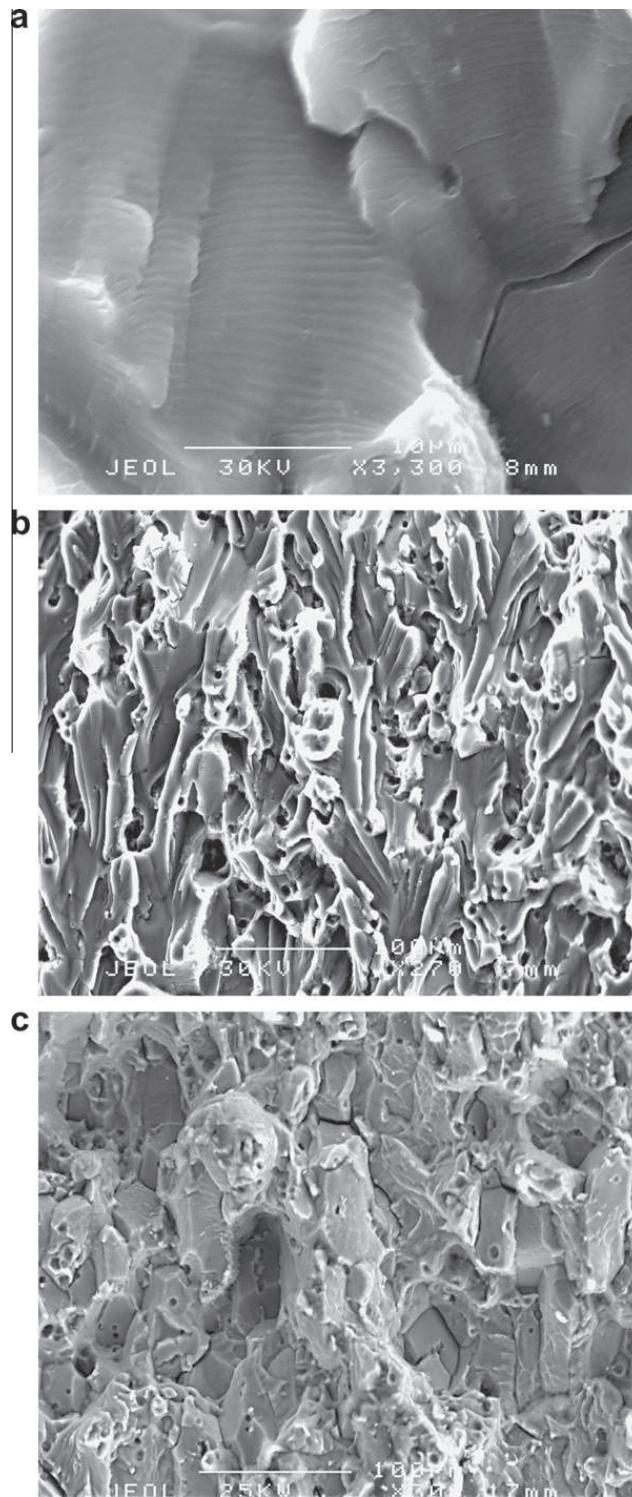
Fig. 10. Fracture surfaces produced during fatigue crack growth in the 2650 T6 alloy (a) at $\Delta K = 9$ MPa m$^{1/2}$, 20 °C, 20 Hz, (b) at $\Delta K = 9$ MPa m$^{1/2}$, 130 °C, 20 Hz, and (c) at $\Delta K = 7$ MPa m$^{1/2}$, 175 °C, 0.05 Hz.

It is noteworthy that, in the T851 ageing condition in the S-L orientation or the L-T orientation in the T351 temper, the facets are much less numerous [16], while these conditions corresponds to a much higher resistance to intergranular SCC cracking. Consistently, the corrosion-assisted 2nd power-law regime is not observed in these conditions. This provides an additional support for the intergranular nature of these facets and for a relation between the SCC susceptibility of 2XXX aluminium alloys and a pronounced FCG enhancement in saline solution: this is due to the orientation between the load direction and the grain orientation on one hand, and the presence of a continuous anodic network along the grain boundaries determined by ageing conditions on the other hand. It has been proposed that the observed crack growth enhancement is
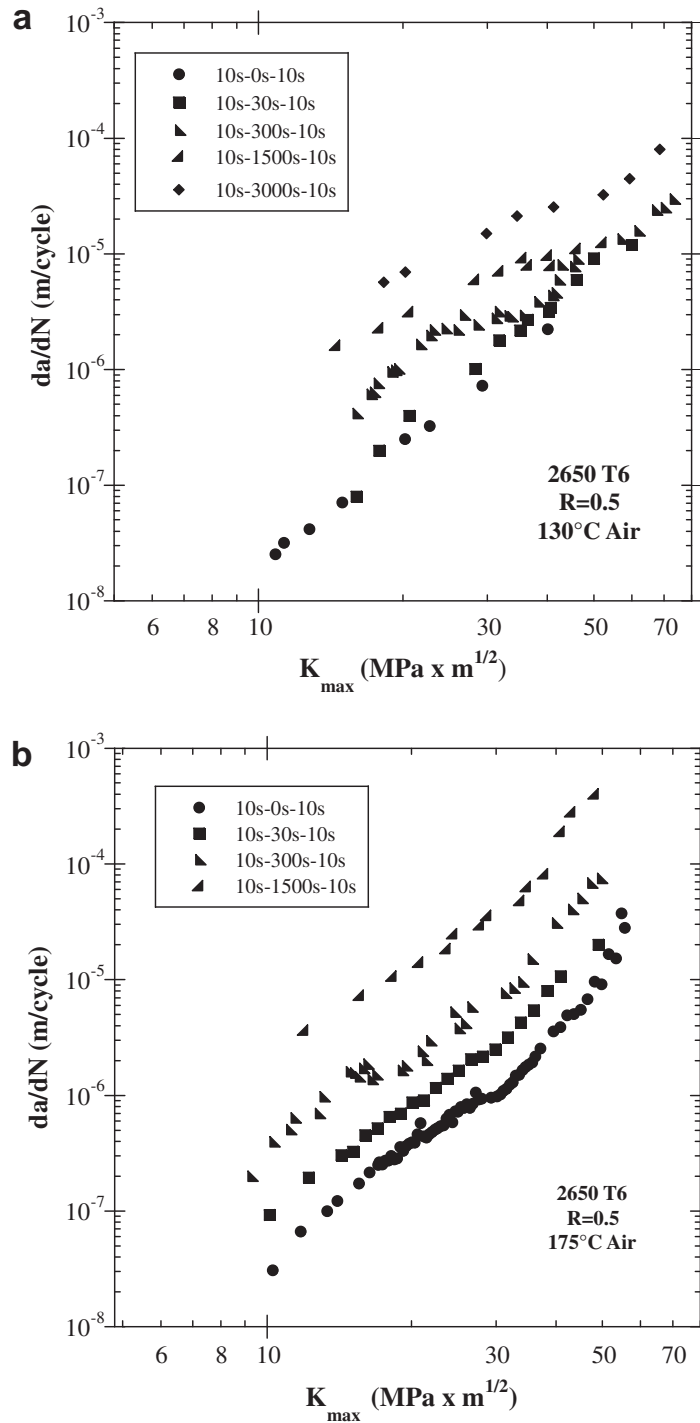
Fig. 11. Influence of hold time on creep–fatigue crack growth rates in the 2650 T6 alloy at $R = 0.5$ (a) at 130 °C and (b) at 175 °C.

related to the entry of a high concentration of hydrogen produced by severe localised dissolution prior to repassivation of the crack tip surfaces into the crack tip [15,16]. Therefore, grain boundary dissolution would be necessary to generate hydrogen but it would not directly control crack propagation along grain boundaries. A similar mechanism has been proposed to account for intergranular stress corrosion cracking in a pure Al–5 Mg alloy [18].

2.3. Conclusion

It has been shown that a significant fraction of fracture surfaces is occupied by intergranular facets as soon as a corrosion-assisted crack growth mechanism is activated. A relation between stress corrosion cracking sensitivity and corrosion-assisted crack growth mechanism can thus be established.
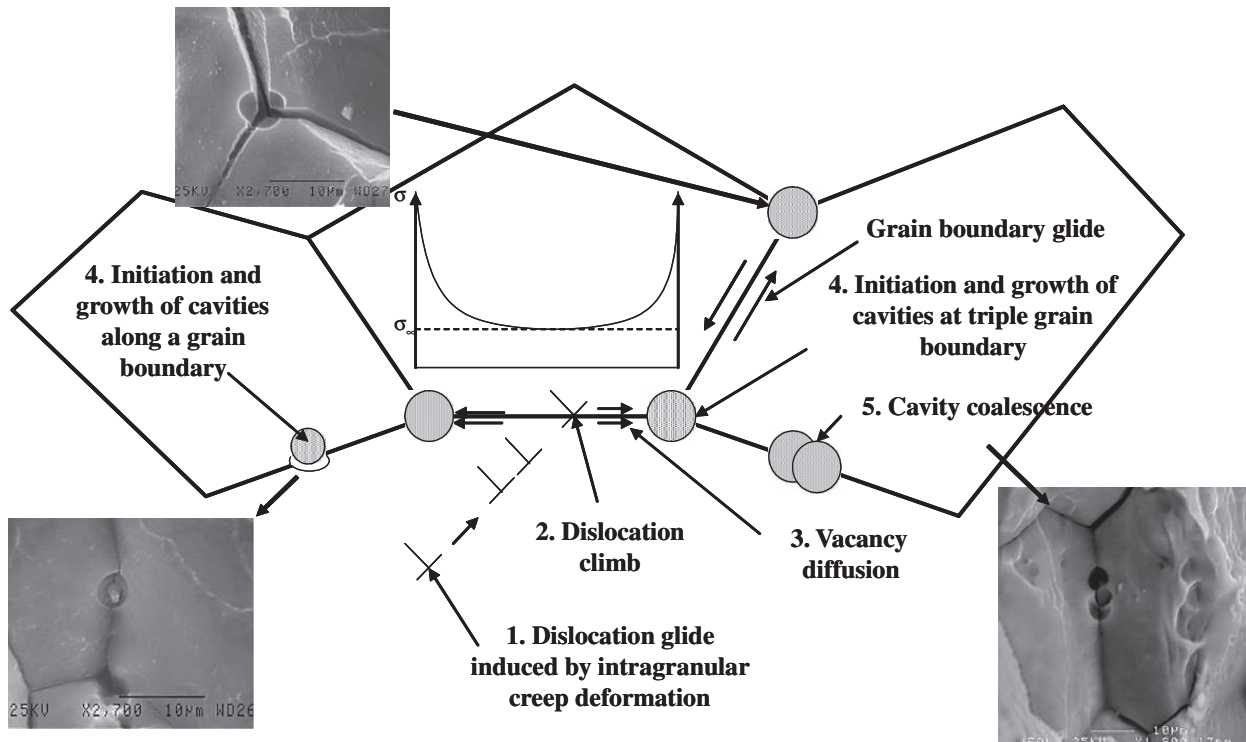
Fig. 12. Mechanisms of intergranular decohesions induced by vacancy diffusion along grain boundaries.

3. Creep–Fatigue Crack Growth in 2650 alloy

3.1. Material and experimental techniques

The 2650 alloy is a copper–magnesium aluminium alloy, provided in the form of sheets by Rhénalu (thickness: 2.5 and 5 mm). The Creep Crack Growth (CCG), Fatigue Crack Growth (FCG) and Creep–Fatigue Crack Growth (CFCG) resistance of this alloy was investigated after T6 artificial ageing treatment (192 °C for 21 h) resulting into a fully recrystallised microstructure with an average grain size of 40 μm in the rolling plane. CCG, FCG and CFCG testing were performed on CT specimens (W = 32 mm) of 5 mm thickness in the L-T orientation. The crack length was monitored by means of the potential drop technique for the three test types. FCG and CFCG were conducted by means of a servo-hydraulic machine equipped with a furnace, using a constant load ratio R = 0.5. The same load ratio was used during tests in vacuum, which were carried out through a servo-hydraulic machine equipped with a furnace and a chamber allowing a residual pressure of about 10^{-7} mbar. Additional information are available in Refs. [19–22].

3.2. Results and analysis

The FCG behaviour of the 2650 T6 alloy at different temperatures and frequencies is presented in Fig. 9. It can be seen that this behaviour is almost unaffected by temperature as far as the frequency is high enough. Consistently the fracture surfaces are not fundamentally influenced by temperature, except for the highest temperature (175 °C) and lowest frequency (0.05 Hz). Indeed, while at 20 °C and 130 °C a cleavage-like fracture surface with the presence of striations is prevailing (Fig. 10a), a substantial amount of intergranular facets is noticed at 175 °C, although the growth rates are not substantially modified (Fig. 10b).

The CFCG rates measured under trapezoidal load signal with different hold time duration are presented for a test temperature equal to 130 °C (Fig. 11a) and equal to 175 °C (Fig. 11b). It can be seen that the introduction of hold time induces a significant crack growth enhancement and that this enhancement is more pronounced as the test temperature is raised. This behaviour is indicative of a possible additional damage mechanism induced by creep. Fracture surface observations are therefore expected to provide further insights onto this issue. Indeed the creep crack growth resistance was previously examined [19], and it was shown that CCG fracture surfaces exhibit two characteristic failure modes: an intergranular fracture mode prevailing in the slow growth rate regime (Fig. 13a) as commonly observed in CCG in these alloys [23], and a mixture of intergranular and ductile fractures before failure. The intergranular mode occurs by cavitation controlled by vacancy diffusion along grain boundaries [24,25], as is shown in Fig. 12. Indeed CFCG fracture surfaces also exhibit significant amounts of intergranular decohesions. Fig. 13b and c presents details observed at higher magnification of this intergranular cavitation process for CFCG.
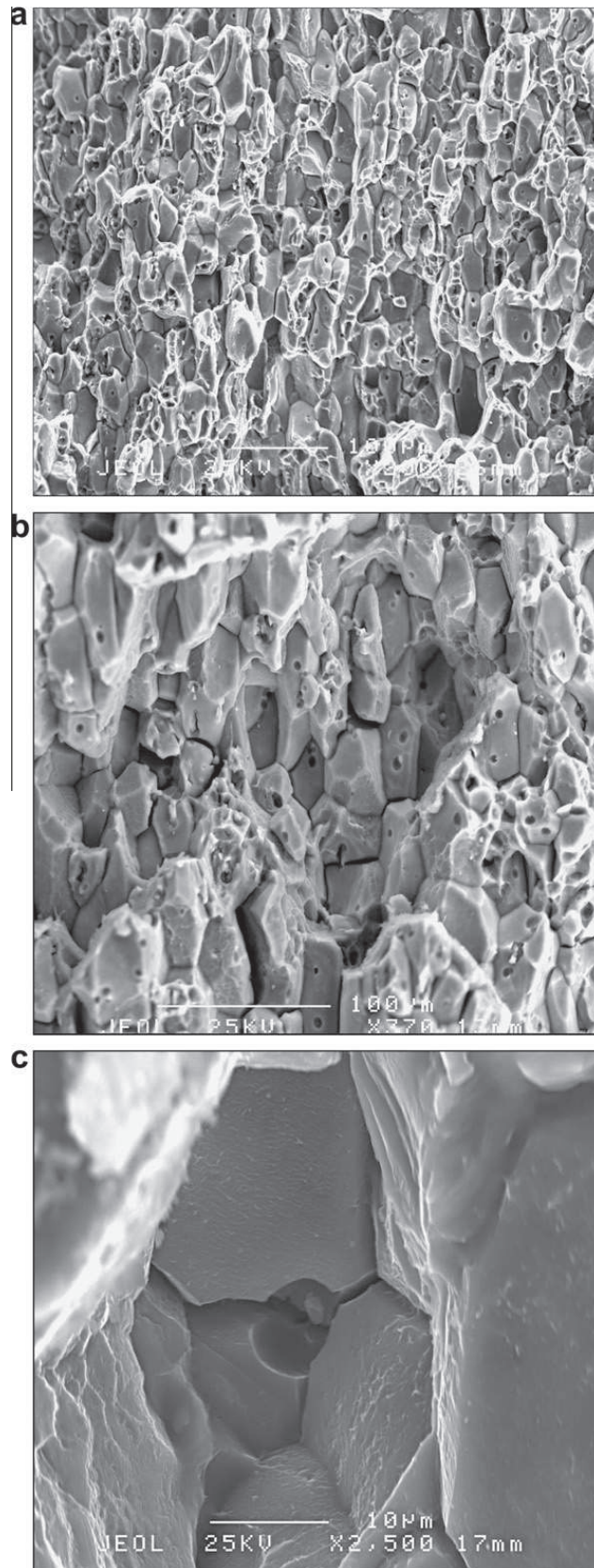
Fig. 13. Fracture surfaces produced in the 2650 T6 alloy during (a) CCG ($K = 22$ MPa m$^{1/2}$, 175 °C), (b) CFCG ($K_{max} = 23$ MPa m$^{1/2}$, $da/dN = 2 \times 10^{-5}$ m/cycle, 10 s–1500 s–10 s, 175 °C) intergranular and ductile rupture ($K = 44$ MPa m$^{1/2}$, 175 °C), and (c) cavitation at triple grain boundary ($K_{max} = 30$ MPa m$^{1/2}$, $da/dN = 2 \times 10^{-6}$ m/cycle, 10 s–300 s–10 s, 175 °C).

In order to analyse the observed crack growth enhancement, quantitative measurements of the area fraction occupied by intergranular facets have been performed for different loading conditions. The results obtained under trapezoidal wave
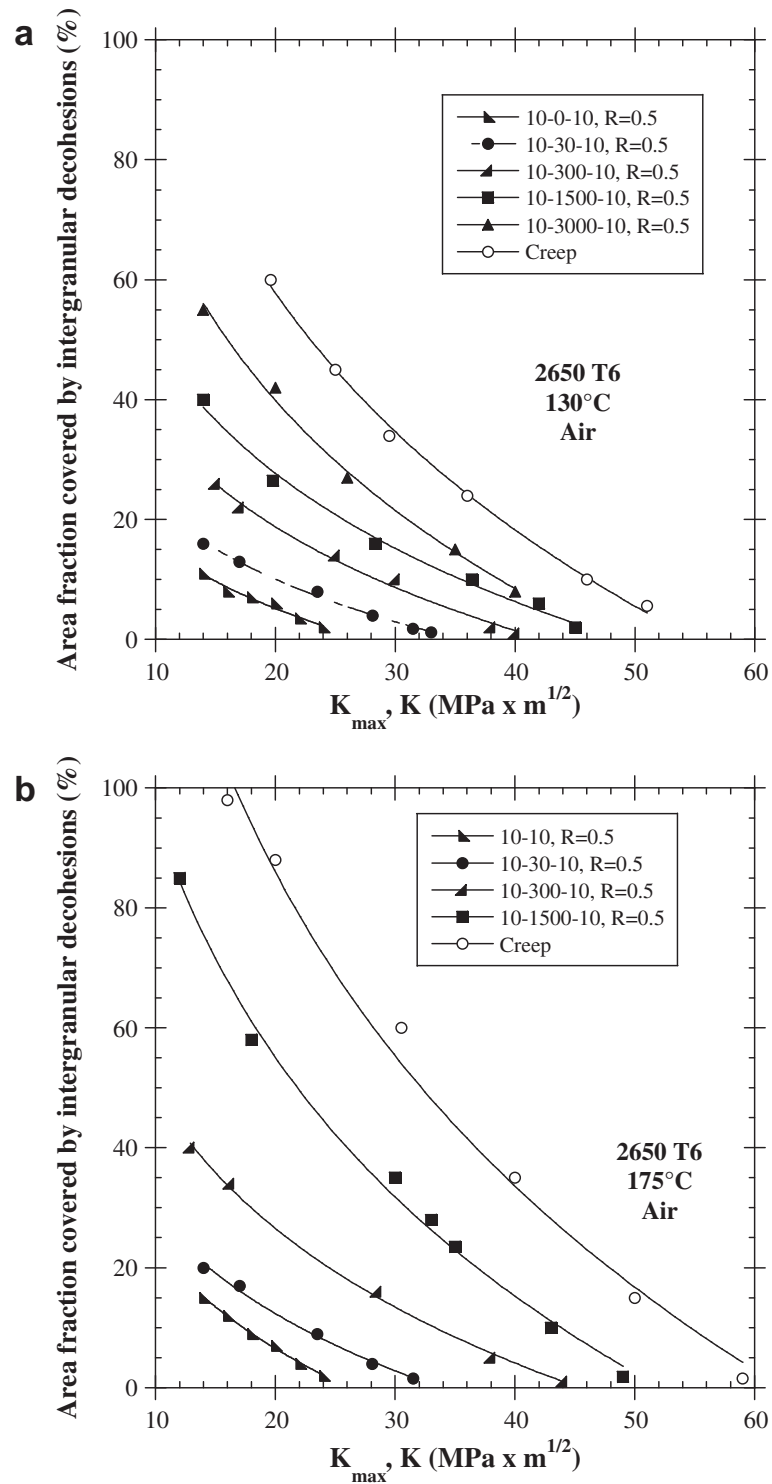
Fig. 14. Percentage of area covered by intergranular decohesions as a function of maximum stress intensity factor for different loading cases (a) at 130 °C and (b) at 175 °C.

shape signals at 130 °C and 175 °C are presented in Fig. 14a and b, respectively, as a function of hold time. It can be noticed that, for a selected temperature, the longer the hold time, the higher the amount of intergranular facets, especially at low K values. Nevertheless, even for hold times as high as 3000s, the amount of intergranular facets never exceeds the amount obtained during CCG at the same K or K_{max} value for a fixed temperature. Besides, for a given hold time value, the percentage of intergranular facets is higher at 175 °C than at 130 °C. Therefore, a relationship between the amount of intergranular decohesions and the crack growth enhancement induced by creep damage with respect to fatigue at high frequency can be established.
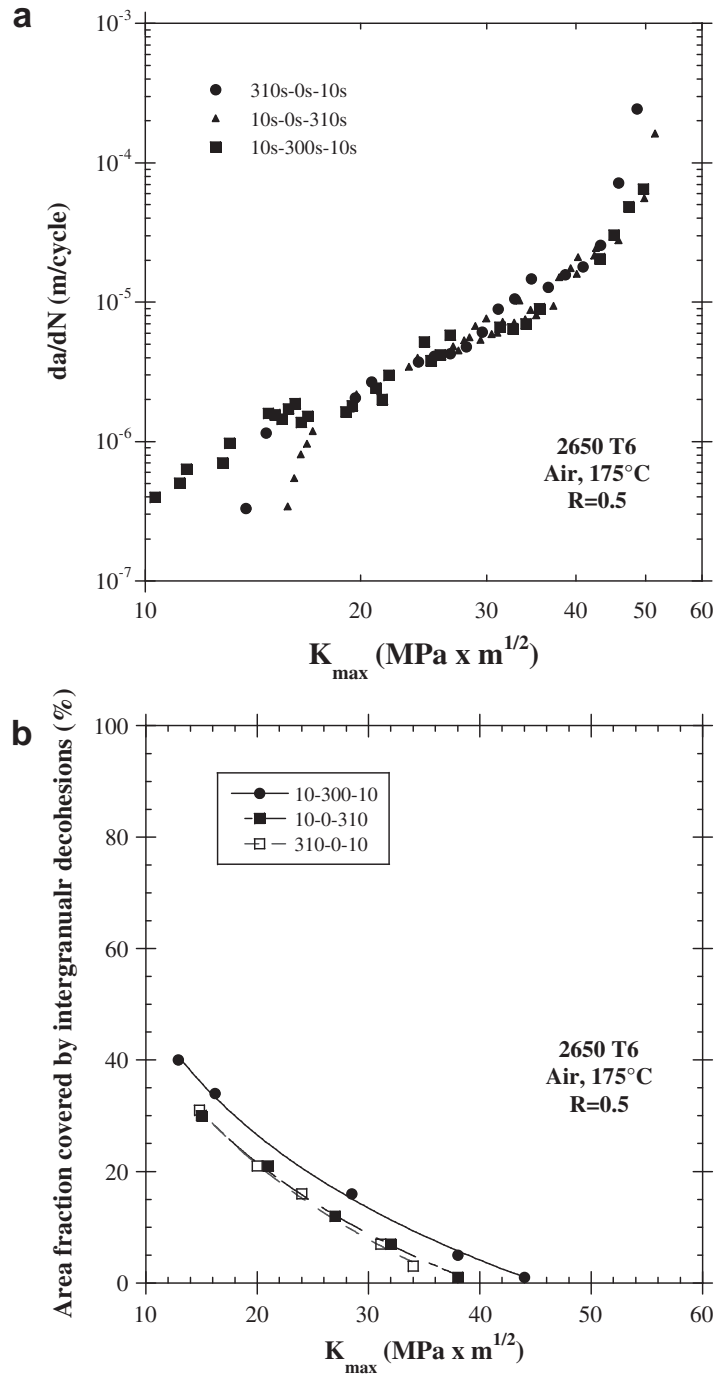
Fig. 15. (a) CFCG rates for three different wave shapes of same period (10 s–300 s–10 s, 10 s–310 s, 310 s–10 s) in air at 175 °C and (b) percentage of area covered by intergranular decohesions for these different loading wave shapes.

An additional support is provided by the results obtained under different wave shapes. Fig. 15a compares the growth rates measured under three different loading wave shapes, namely positive and negative saw tooth signal and a trapezoidal signal with the same period, namely 320 s. It can be seen that, except at low K_{max} values, the data fall onto a single curve, suggesting that the observed enhancement is mainly controlled by the load period, and not by the loading rate or the hold time. The corresponding percentages of intergranular fracture, reported in Fig. 15b, are consistent with the growth rate data, despite of a slight discrepancy between saw tooth results on the one hand and trapezoidal signal on the other hand. One can thus consider that a unique relation exists between a selected value of the load period on the one hand, and the growth rate and the amount of intergranular fracture on the other hand. However, it should be stressed that such a relation only stands for a fixed environment, namely air. Indeed it has been shown that environment can modify the creep–fatigue growth rates as well as the percentage of intergranular facets [20].

3.3. Summary

Intergranular decohesions induced by vacancy diffusion control both creep crack growth and fatigue crack growth at low frequencies and elevated temperatures, as far as the 2650 T6 alloy is concerned. As regards crack growth under cyclic loading at low frequency, it has been shown that the amount of intergranular facets can be related to the load period and, as a consequence, to the crack growth enhancement during cyclic loading at low frequencies.

4. Conclusions

The present paper shows evidences of intergranular crack paths that are produced under cyclic loading in 2XXX AA as soon as time-dependent processes, such as corrosion or creep, take place at the crack tip. However, at least in the cases considered here, the fracture surface is rarely entirely intergranular. Grain boundaries rather seem to constitute a preferential crack path, presumably due to the high concentration along these boundaries of trapped hydrogen or vacancies, depending on the time-dependent process involved. Therefore, if a significant amount of intergranular fracture is associated to a crack growth enhancement, it does not mean that intergranular fracture per se is faster than transgranular propagation, but it is rather indicative of an additional damage mechanism taking place during crack growth. Such issues, when relevant, should be taken into account by applying advanced models for fatigue crack propagation (for instance those based on cohesive zone models).

References

[1] Forsyth PJE. Fatigue damage and crack growth in aluminium alloy. Acta Metall 1963;11:703–15.
[2] Petit J, Kosche K, Gudladt HJ. Intrinsic stage I crack propagation in Al–Zn–Mg single crystals. Scripta Metall Mater 1992;26:1049–54.
[3] Laird C. The influence of metallurgical structure on the mechanisms of fatigue crack propagation 1967. Fatigue Crack Propagation, ASTM STP 415 ASTP, p. 131–80.
[4] Petit J, Henaff G. A survey of near-threshold fatigue-crack propagation – mechanisms and modeling. Fatigue 93 1993;1–3:503–12.
[5] Slavik DC, Gangloff RP. Environment and microstructure effects on fatigue crack facet orientation in an Al–Li–Cu–Zr alloy. Acta Mater 1996;44(9):3515–34.
[6] Henaff G, Marchal K, Petit J. On fatigue crack propagation enhancement by a gaseous atmosphere: experimental and theoretical aspects. Acta Metall Mater 1995;43(8):2931–42.
[7] Frandsen JD, Marcus HL. The correlation between grain size and plastic zone size for environmental assisted fatigue crack propagation. Scripta Metall 1975;9:1089–94.
[8] Clark G, Pickard AC, Knott JF. A note on the effects of stress intensity and frequency on the occurence of intergranular facets during the fatigue of a low-alloy steel. Engng Fract Mech 1976;8:449–51.
[9] Ritchie RO. Contribution on "Slow fatigue Crack Growth and Threshold Behaviour of a Medium Carbon Steel in Air and in vacuum" by R. J. Cooke, P. E. Irving, G. S. Booth and C. J. Beevers. Engng Fract Mech 1975;7:187–9.
[10] Hénaff G, Petit J. Environmentally-assisted fatigue crack propagation: some critical issues. In: Lutjering G, Nowack H, editors. Fatigue'96. Berlin (Germany): Pergamon; 1996. p. 715–20.
[11] Kobayashi S, Inomata T, Kobayashi H, Tsurekawa S, Watanabe T. Effects of grain boundary- and triple junction-character on intergranular fatigue crack nucleation in polycrystalline aluminum. J Mater Sci 2008;43(11):3792–9.
[12] Feeney JA, McMillan JC, Wei RP. Environmental fatigue crack propagation of aluminum alloys at low stress intensity levels. Metall Trans 1970;1(6):1741.
[13] Gangloff RP. Environment sensitive fatigue crack tip processes and propagation in aerospace aluminum alloys. In: Blom AF, editor. Fatigue '02 international fatigue congress. West Midlands (UK): Engineering Materials Advisory Services; 2002. p. 3401–33.
[14] Gingell ADB, King JE. The effect of frequency and microstructure on corrosion fatigue crack propagation in high strength aluminium alloys. Acta Mater 1997;45(9):3855–70.
[15] Menan F, Henaff G. Influence of frequency and waveform on corrosion fatigue crack propagation in the 2024–T351 aluminium alloy in the S-L orientation. Mater Sci Engng, A 2009;519(1–2):70–6.
[16] Menan F, Henaff G. Influence of frequency and exposure to a saline solution on the corrosion fatigue crack growth behavior of the aluminum alloy 2024. Int J Fatigue, Fatigue Damage Struct Mater VII 2009; 31 (11–12): 1684–95.
[17] Lynch SP. Mechanisms of hydrogen assisted cracking – a review 2003. In: Jones RH, editor. Hydrogen effects on material behavior and corrosion deformation interactions. Minerals, Metals & Materials Soc: Warrendale (PA). p. 449–66.
[18] Tanguy D, Bayle B, Dif R, Magnin T. Hydrogen effects during IGSCC of pure Al–5Mg alloy in NaCl media. Corros Sci 2002;44(6):1163–75.
[19] Odemer G, Henaff G, Journet B. Creep crack growth resistance of an age hardened aluminium alloy for supersonic applications. Scripta Mater 2006;54(1):51–5.
[20] Henaff G, Odemer G, Tonneau-Morel A. Environmentally-assisted fatigue crack growth mechanisms in advanced materials for aerospace applications. Int J Fatigue 2007;29(9–11):1927–40.
[21] Odemer G, Hénaff G, Journet B, Rémy L. Creep–fatigue interactions during crack growth in a 2650 T6 aluminium alloy. In: Johnson S, McDowell DL, Newman Jr JC, Saxena A, editors. Fatigue'2006, 9th international congress on fatigue. Atlanta (Georgia, USA): Elsevier; 2006.
[22] Henaff G, Odemer G, Benoit G, Koffi E, Journet B. Prediction of creep–fatigue crack growth rates in inert and active environments in an aluminium alloy. Int J Fatigue, Fatigue Damage Struct Mater VII 2009; 31 (11–12): 1943–51.
[23] Bensussan PL, Jablonski DA, Pelloux RM. A study of creep crack-growth in 2219-T851 aluminum-alloy using a computerized testing system. Metall Trans A – Phys Metall Mater Sci 1984;15(1):107–20.
[24] Yang L. Study of creep crack growth in 2618 and 8009 aluminum alloys. Metall Mater Trans A 1995;26(2):315–28.
[25] Vitek V. A theory of diffusion controlled intergranular creep crack growth. Acta Metall 1978;26(9):1345–56.